



# The microstructure of the interfacial transition zone between steel and cement paste

Li Yue<sup>a,\*</sup>, Hu Shuguang<sup>b</sup>

<sup>a</sup>State Key Laboratory of Concrete Materials Research, Tongji University, Shanghai 200092, People's Republic of China

<sup>b</sup>Wuhan University of Technology, Wuhan 430070, People's Republic of China

Received 3 March 2000; accepted 11 December 2000

## Abstract

The microstructures of steel/ordinary paste and steel/expansive paste interfaces were investigated. The  $\text{Ca}(\text{OH})_2$  orientation effect, the crystal sizes of  $\text{Ca}(\text{OH})_2$  and Aft, the morphologies and the relative percentages of the Si, Al, S and Ca elements of interfaces were specially studied. The results show that, under confined conditions, the microstructure of the steel/expansive paste interface is better than that of the steel/ordinary paste interface. © 2001 Elsevier Science Ltd. All rights reserved.

**Keywords:** Interfacial transition zone; Microstructure; Confined condition; Expansion; Cement paste

## 1. Introduction

Experimental research [1–3] indicates that the microstructure of the transition zone between aggregate and cement paste is important for the strength and durability of concrete. Likewise, the microstructure of the transition zone between steel and cement paste also obviously influences the properties of steel/concrete composites (such as concrete-filled steel tube). At present, studies of the steel/paste interface mostly focus on ordinary cement paste. The results generally show that the transition zone between steel and paste exists, and its microstructure is weak, and  $\text{Ca}(\text{OH})_2$  crystals tend to be present in the transition zone [4–7]. However, up to now, few studies on steel/expansive paste have been done.

## 2. Experimental

### 2.1. Raw materials

Number 525 ordinary Portland cement and expansive agent UEA made of raw alum earth and gypsum were used. Their chemical compositions are shown in Table 1.

\* Corresponding author. Tel.: +86-21-6598-3463; fax: +86-21-6598-5680.

E-mail address: liyue@mail.east.sh.cn (L. Yue).

### 2.2. Methods

As shown in Fig. 1, the pure cement paste and the expansive paste (12 wt.% UEA was substituted for cement) were cast in small steel tubes  $\emptyset 26 \times 3 \times 20$  mm (diameter  $\times$  wall thickness  $\times$  height). The water to binder ratios of both kinds of paste are 0.28. A stainless-steel disc was inserted in the paste. The specimens were cured within the small steel tube until the testing ages in standard condition ( $20^\circ\text{C}$ , RH  $95 \pm 5\%$ ). During the curing period, a steel block was put on top of the steel tube to ensure curing under confined conditions. The following method of preparing the steel/paste interface was employed: The hardening paste was jacked out of the steel tube and broke off at the position of the steel disc, thus, the interface was obtained. The matrix surface was obtained by polishing the sample interface. The samples to be tested were kept in ethyl alcohol to avoid carbonization and rehydration.

Table 1  
Chemical compositions of raw materials (wt.%)

Material	$\text{SiO}_2$	$\text{Al}_2\text{O}_3$	$\text{Fe}_2\text{O}_3$	CaO	MgO	$\text{SO}_3$	Loss
Cement	21.47	5.80	4.04	59.64	3.24	2.08	2.44
UEA	29.50	7.76	2.82	17.93	1.83	24.79	20.67

### 3. Results and discussion

#### 3.1. The orientation index of $\text{Ca}(\text{OH})_2$ in the interface

The preferential orientation of crystal refers to the fact that some crystal lattices or crystal edges have a prior development or arrangement in a certain direction. The preferential orientations remarkably affect the properties of materials. In the steel/cement interface, whether or not  $\text{Ca}(\text{OH})_2$  was oriented and its orientation degree can be judged by the orientation index  $I$ . The definition of the orientation index  $I$  is as follows:

$$I = \frac{R}{R_0} = \frac{I'(001)/I'(101)}{0.74} \quad (1)$$

where  $R = I'(001)/I'(101)$ .  $I'(001)$  and  $I'(101)$  specially are the diffraction strength of the (001) and (101) faces of  $\text{Ca}(\text{OH})_2$  crystal. For nonorientated  $\text{Ca}(\text{OH})_2$ ,  $R = R_0 = 0.74$ . The orientation index  $I$  could illustrate the distribution of  $\text{Ca}(\text{OH})_2$  in the transition zone. If  $I > 1$ ,  $\text{Ca}(\text{OH})_2$  is oriented. The larger  $I$  is, the larger the amount of oriented  $\text{Ca}(\text{OH})_2$  is. When  $I = 1$ , no orientation occurs. In our experiment, X-rays are directly irradiated on the interface and the matrix surface. With the XRD patterns of different samples, the orientation index  $I$  could be calculated by Eq. (1), and the results are shown in Fig. 2.

The results suggest that the  $\text{Ca}(\text{OH})_2$  in the matrix of ordinary and expansive paste is not oriented, the orientation indices basically being 1.0. The  $\text{Ca}(\text{OH})_2$  crystal in both kinds of interfaces are oriented with its plane (001) parallel to the interface. However, the orientation indices of expansive paste at different hydration ages are lower than that of ordinary paste, which revealed that the  $\text{Ca}(\text{OH})_2$  growth situation in the interface of steel/expansive paste was improved under confined condition, compared to that of ordinary paste.

#### 3.2. The crystal size of CH and AFt in the interfaces

The crystal size relates to the crystal growth space. When the growth space is larger, the confinement of crystal

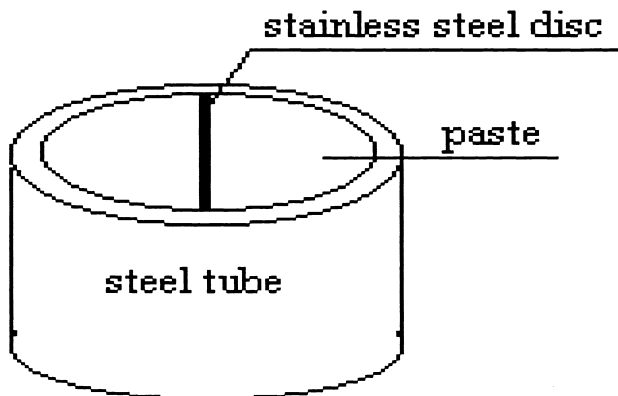


Fig. 1. Layout of paste shaping.

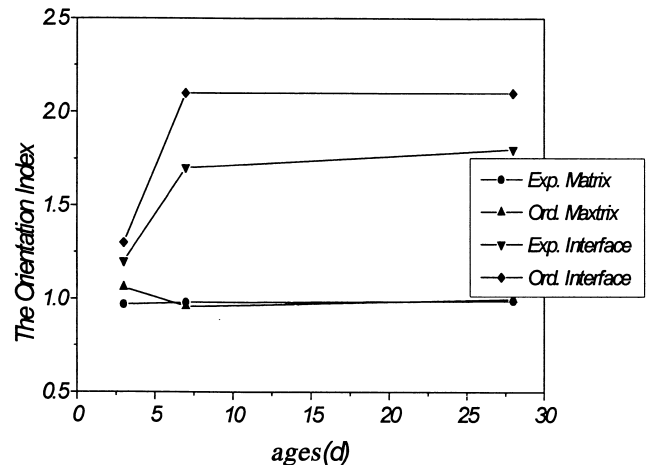


Fig. 2. The orientation index of  $\text{Ca}(\text{OH})_2$ .

growth is smaller, and, thus, the crystal size is larger. Therefore, the crystal size can illustrate the structure of the porosity, which can also demonstrate the characteristics of the transition zone. Many methods can be used to measure the crystal size: XRD methods, optical microscope analyses and SEM analyses. Compared to other methods, XRD methods are suitable for cement paste due to its complicated microstructure. In our experiment, the XRD method was used. The calculation of crystal size is based on Scherrer equation (Eq. (2)):

$$D = \frac{k\lambda}{\beta \cos \theta} \quad (2)$$

where  $D$  is the average crystal size,  $\lambda$  the wavelength of X-ray,  $k$  a constant and is approximately equal to 1,  $\theta$  the Bragg angle between X-ray and crystal face and  $\beta$  the width of diffraction peak. The calculation processes were finished through a ready-made computer program, and the results are shown in Figs. 3 and 4.

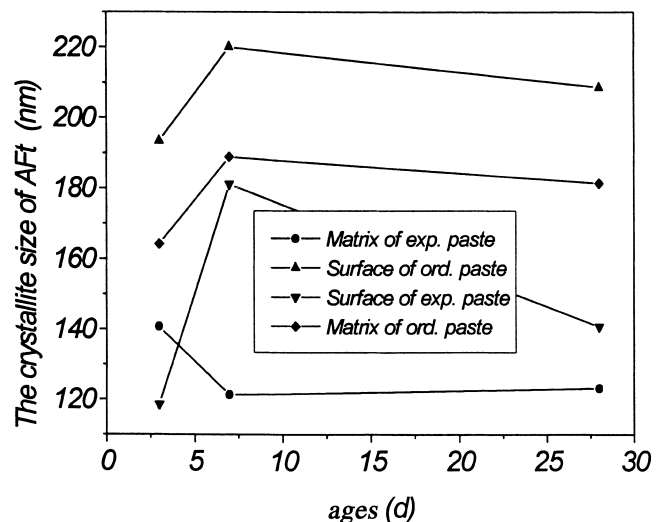


Fig. 3. The crystallite size of AFt(110).

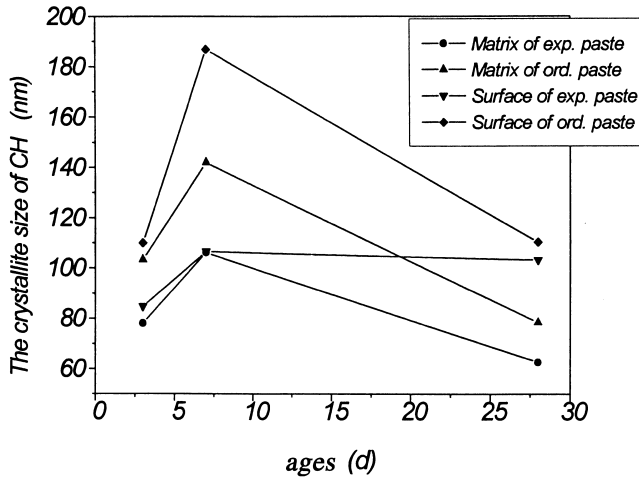


Fig. 4. The crystallite size of  $\text{Ca(OH)}_2(101)$ .

It can be seen from Figs. 3 and 4 that, under confined conditions, the  $\text{Ca(OH)}_2$  and AFt crystal sizes of expansive paste both in the interface and in the matrix were smaller than that of ordinary paste. The results illustrate that the microstructure of expansive paste was improved.

### 3.3. SEM (EDXA) analyses on the interface

For further study, the mineralogy and microstructure of the interface, SEM (EDXA) analyses were employed. Fig. 5 shows SEM photos of the interfaces between steel and hardening paste at 28 days.

With SEM analyses, we found that it was hard to find plane-like CH and needle-like AFt in the interface of expansive paste at early hydration, and a lot of gelatinous hydrate existed in the interface. However, a large amount of CH and AFt existed in the interface of ordinary paste. During the later hydration, the gelatinous hydrate of expansive paste became more and more dense; the CH and AFt crystals were hard to find and many cracks and holes appeared in the interface of the ordinary paste. These observation reveals that the microstructure at the steel/expansive paste interface is better than that of ordinary paste under confined condition. The reason why the interface microstructure of steel/expansive paste was improved is the same as that of aggregate/expansive paste [8] and can be explained as follows. During the early hydration, a large amount of water fills around the steel face to form a water film due to inner bleeding in fresh paste. For ordinary paste, the paste will shrink, which provides rather large space between the steel/paste interfaces. Compared with  $\text{SiO}_4^{2-}$ , ions  $\text{Ca}^{2+}$ ,  $\text{SO}_4^{2-}$  and  $\text{Al}^{3+}$  have rather high diffusion speed and can easily penetrate into the water film by diffusion. When these ions reach the oversaturation condition, they will crystallize and grow to form large crystal. Therefore, a large amount of CH and AFt were present in the interface at early hydration. With the curing time prolonging, other

hydration products such as C-S-H gel will gradually form and cover or fill around the early-formed AFt and CH. Therefore, it was hard to find CH and AFt crystal. At this period, however, autogenous shrinkage is the main shrinkage type of ordinary paste with low w/c and under no water curing condition [9]. As a result, cracks and holes appeared in the interface. For expansive paste under confined condition, the volume expansion of paste will reduce the thickness of water film and make the paste come close to the steel face, which causes the cement hydration products such as C-S-H gel to have more opportunities to connect with steel face. The contact is effectively increased with the curing time prolonging. Moreover, the reduction of crystal growth space limited the free growth of AFt and CH. Therefore, instead of large CH and AFt crystal, the main components in the interface zone are dense C-S-H gel and fine AFt crystal.

In addition, EDXA was used to analyse the weight percentages of main elements at the interfaces. The results are shown in Table 2. In the EDXA analysis, the scanned region of every specimen is same, and the enlargement factor is 25 times. Therefore, the results could represent the situation of the elements' weight percentages in the whole interface.

It can be seen in Table 2 that, because of UEA replacing part of the cement, the weight percentages of elements Al,

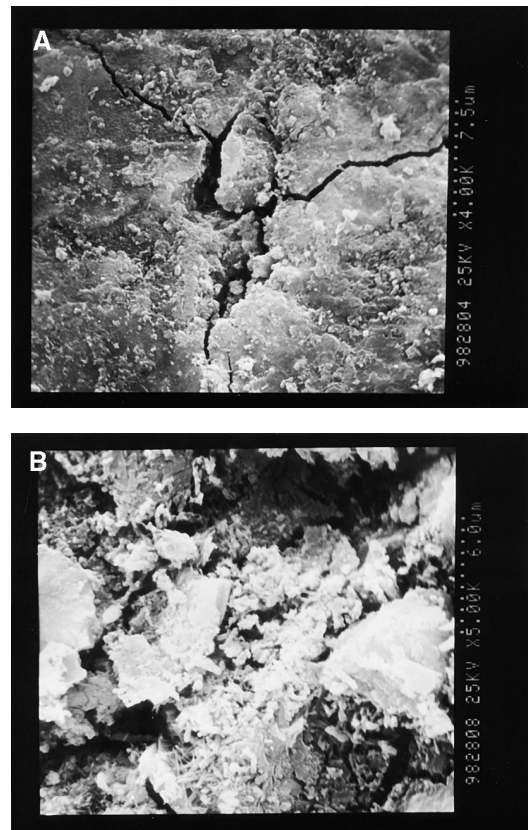


Fig. 5. The SEM photos of interface zone of two kinds of paste at 28 days. A: Ordinary paste; B: Expansive paste.

Table 2  
The relative percentage of main elements in interface zone (wt.%)

Elements	Expansive (3 days)	Ordinary (3 days)	Expansive (28 days)	Ordinary (28 days)
Al	4.86	3.62	5.13	2.96
Si	15.60	13.74	10.90	10.87
S	5.07	2.23	5.22	2.27
Ca	74.47	80.41	78.75	83.90

Si and S at the expansive paste interface are higher than those in the ordinary paste, and the element Ca is lower than that in the ordinary paste. The increase in weight percentage of element Si is beneficial to form C-S-H gel to improve the interface microstructure.

#### 4. Conclusions

(1) The preferential orientation of CH crystals takes place in the interface of steel/ordinary paste and steel/expansive paste. However, the orientation indices of CH in the expansive paste interface at different hydration ages are always lower than those of the ordinary paste under confined conditions.

(2) Under confined conditions, the CH and Aft crystal sizes of expansive paste both in the interface and in the matrix are smaller than those of the ordinary paste, which illustrates that the microstructure of the expansive paste is improved.

(3) Compared to the ordinary paste, the gelatinous hydrate volume in the interface of expansive paste is

large and the interface microstructure is closer and more even, and the weight percentage of element Si is higher, which is beneficial to the formation of C-S-H gel. Therefore, the microstructure of steel/expansive paste is much better than that of steel/ordinary paste under confined conditions.

#### References

- [1] R. Zimbelman, Contribution of cement–aggregate bond, *Cem. Concr. Res.* 15 (5) (1985) 801–808.
- [2] D.P. Bentz, P.E. Stutzman, E.J. Garboczi, Experimental and simulation studies on the interfacial zone in concrete, *Cem. Concr. Res.* 22 (5) (1992) 891–902.
- [3] B. Dannels, B. Gerard, G. Jacpues, Contribution to formation mechanism of the transition zone between rock–cement paste, *Cem. Concr. Res.* 23 (2) (1993) 335–346.
- [4] D.J. Pinchin, D. Tabor, Interfacial phenomena in steel fiber reinforced cement: I. Structure and strength of interfacial region, *Cem. Concr. Res.* 8 (1) (1978) 15–24.
- [5] C.L. Page, M.N. Al. Khalaf, A.G.B Ritchie, Steel/mortar interfaces: mechanical characteristics and electrocapillarity, *Cem. Concr. Res.* 8 (3) (1978) 481–490.
- [6] C. Tashiro, S. Tatibana, Bond strength between  $C_3S$  paste and iron, copper or zinc wire and microstructure of interface, *Cem. Concr. Res.* 13 (2) (1983) 373–382.
- [7] P.J.M. Monteiro, O.E. Gjorv, P.K. Mehta, Microstructure of the steel–cement paste interface in the presence of chloride, *Cem. Concr. Res.* 15 (5) (1985) 781–784.
- [8] S. Hu, Y. Li, Research on hydration, hardening mechanism, and microstructure of high performance expansive concrete, *Cem. Concr. Res.* 29 (7) (1999) 1013–1017.
- [9] E. Tzazwa, *Autogenous Shrinkage of Concrete*, E&FN Spon Press, New York, 1998.